SEISMIC DESIGN AND DUCTILITY EVALUATION OF STEEL TUBULAR BRIDGE PIERS WITH GRADED THICKNESS

I.H.P. Mamaghani[(1)]

[(1)] *Associate Professor, Department of Civil Engineering, University of North Dakota, iraj.mamaghani@und.edu*

Abstract

This paper deals with the hysteretic behavior of uniform (BB) and proposed graded-thickness (BGB) thin-walled steel bridge piers of square box columns under constant axial force and circular bidirectional cyclic lateral loading. First, the adopted finite element model (FEM) is verified with the experimental results in the literature using commercial computer program ABAQUS that was employed for the analysis. Second, the proposed BGB column, with the same material, cross-section size and volume of material equivalent to the BB column, is evaluated. Then, the strength and ductility deterioration of the column under circular bidirectional cyclic loading path over the unidirectional path is emphasized. Finally, an intensive parametric study is conducted to investigate the effect of main design parameters including: flange width-to-thickness ratio parameter (R_f), column slenderness ratio parameter (λ), magnitude of axial load (P/P_y), and number of loading cycles (N) on the overall hysteretic behavior of BB and BGB columns under constant axial force and circular bidirectional cyclic lateral loading. Subsequently, design formulas have been derived to predict the ultimate strength and ductility of the BB and BGB columns.

Keywords: Thin-Walled Steel Box Section; Graded-Thickness; Bidirectional Cyclic Loading; Seismic Design, Ductility.

1. Introduction

Thin-walled steel stiffened square box columns are employed in a variety of structural applications for their favorable structural and constructional advantages in urban earthquake-prone regions [1–4]. These columns are particularly commonly constructed as a cantilever bridge pier [4] due to high strength-to-weight ratio, aesthetic exposed appearance, and potential for concrete infilling [5]. However, thin-walled steel columns are vulnerable to local buckling under strong earthquakes [6–9]. Local buckling leads to significant strength and ductility degradation, and early full collapse of these columns due to cyclic lateral loading [2,3]. It has been confirmed that the width-to-thickness ratio parameter (R_f) and slenderness ratio parameter (λ) are the two main structural parameters affecting the strength and ductility of thin-walled steel box columns [10,11]. In the reality, the earthquake ground motion is complex and three dimensional (*3D*) loading components acting simultaneously, as opposed to assumed unidirectional loading pattern [12–15]. Moreover, hysteretic behavior of thin-walled steel tubular columns under multidirectional cyclic lateral loading is expected to be more critical and severe than the same amplitude of unidirectional cyclic loading. Recently, the hysteretic behavior of thin-walled steel tubular columns under bidirectional cyclic lateral loading was experimentally investigated by a number of researchers [13,15–17]. The studies revealed that thin-walled steel tubular columns under bidirectional cyclic lateral loading surfer an extensive degradation in strength and ductility compared to unidirectional cyclic lateral loading, and should be incorporated in the seismic design practice [13,18,19]. Along with the R_f and λ; cyclic lateral loading pattern, and magnitude of axial load must be practically considered in the seismic design of the thin-walled steel tubular columns [18].

Up to date, researchers investigated thin-walled steel square box columns with uniform thickness under uni/multidirectional cyclic lateral loading. All these studies addressed that thin-walled steel columns suffer local buckling near the base [2,3,20]. In order to address this limitation and ensure an adequate strength and ductile behavior of thin-walled steel columns, thin-walled steel square box column with graded thickness has been recently proposed and investigated by the authors under constant axial force and

unidirectional cyclic lateral loading [3]. In evaluating the proposed graded-thickness column, its strength and ductility improvement under unidirectional cyclic lateral loading is obvious as the proposed graded-thickness column inhibit the local buckling near the base.

As the main objective of this study, the proposed graded-thickness thin-walled steel square box columns (denoted as BGB in the further text) is evaluated in regard to the strength and ductility under constant axial force and bidirectional cyclic lateral loading. In order to achieve this goal, a thin-walled steel square box column with uniform thickness from the reported literature [12,15] was numerically analyzed under constant axial force and bidirectional cyclic lateral loading to validate the accuracy of the adopted FEM. Then, the proposed BGB column with size and volume of material equivalent to a uniform thin-walled steel square box column (i.e., BB column) is investigated under the same loading amplitude and conditions. The study results indicate the proposed BGB columns are advantageous in achieving significant improvements in ultimate strength and ductility compared to their counterpart BB columns, emphasizing the effect of the plate thickness and sectional configuration in the proposed BGB column. The achieved improvements in the overall behavior of the proposed BGB is due to their ability to inhibit the local buckling near the base of the column. Furthermore, it is found that the hysteretic behavior of BB and BGB columns is more severe and critical under circular bidirectional cyclic lateral loading compared to unidirectional cyclic lateral loading.

2. Finite element Model

In this study, a commercial finite element software ABAQUS 6.14 is employed for the FE analysis where material and geometric nonlinearities are taken into account during computational process [21]. The validity of the adopted FEM is substantiated with the experimental results reported in the literature [12,15]. The main structural parameters in the practical design of thin-walled steel square box columns are R_f and λ. The local buckling is influenced by R_f and λ affects the global buckling behavior [3] which are defined as follows:

$$R_f = \frac{D}{t}\sqrt{\frac{\sigma_y}{E}\frac{12(1-\nu^2)}{\pi^2 k_R}}, \quad k_R = 4n^2 \tag{1}$$

$$\lambda = \frac{2h}{r}\frac{1}{\pi}\sqrt{\frac{\sigma_y}{E}} \tag{2}$$

where h = column height, D = column width, t = plate thickness, r = radius of gyration of cross section, σ_y = yield stress, E = Young's modulus, ν = Poisson's ratio, K_R = buckling coefficient of the subpanel, and n = the number of subpanels for each plate. For the tested column, h = 2420 mm, D = 450 mm, t =6 mm, r = 175 mm, σ_y = 325 MPa, E = 206 GPa, and ν = 0.3 [15]. As shown in Fig. 1, the column is fixed at the base and subjected to constant axial force (P) and bidirectional cyclic lateral displacement at the top. The lower part of the column (2D), which is susceptible to the local buckling, is modeled by reduced integration four-node shell elements (S4R), while the two-node beam element (B31) is employed for the upper part of the column (h-2D). The interface between S4R and B31 elements is linked using multi-point constraint (MPC). For computational efficiency and accuracy, the upper part of the column, height of h-2D, is divided into B31 elements with size of 90 mm.

The bottom portion of the lower part of the column (equal to the width of cross-section, D) is divided into 30 S4R elements, while the remaining height (D) is only divided into 20 elements. Finally, each longitudinal stiffeners and subpanel between the stiffeners, respectively, have 3 and 6 columns of S4R. The above-stated mesh sizes are found to give more efficient and reasonable results. Recent studies concluded that initial geometric imperfection and residual stresses due to welding have insignificant effect on the hysteretic behavior of thin-walled steel columns under cyclic loading [22-25]. Accordingly, the initial residual stresses are not taken into account in this study.

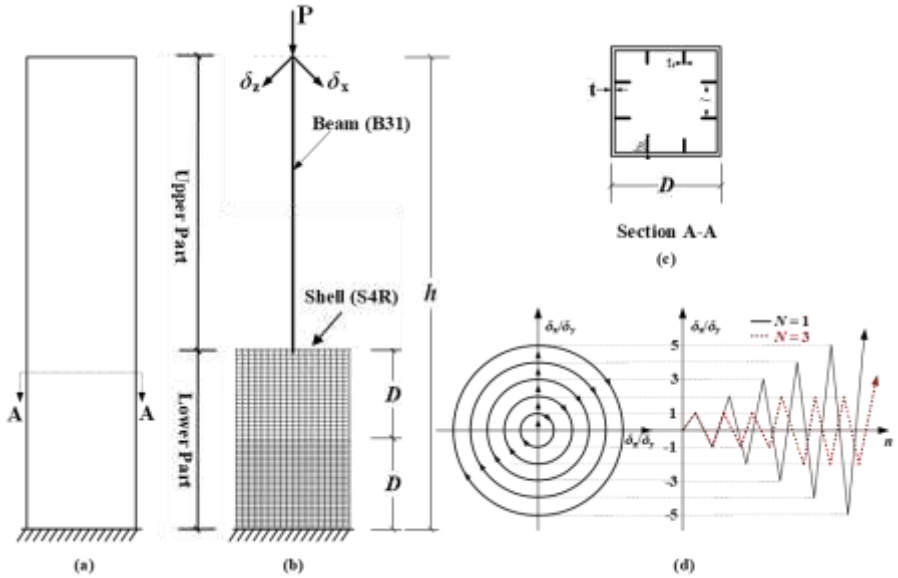

Fig. 1 - Tested Column Model: (a) Column; (b) FE Meshing; (c) Cross Section; and (d) Loading Program.

2.1 Bidirectional Cyclic Loading

As illustrated in Fig. 1d, among several recorded earthquakes ground motions, the displacement-controlled circular cyclic lateral loading is selected as the severest loading path [18]. The adopted quasi-static bidirectional cyclic lateral loading is applied to the top of the column concurrently with a constant axial force (*P*). In each loading step, the amplitude of the cyclic displacement is increased as a multiple of the yield displacement (δ_y), which is defined by:

$$\delta_y = \frac{H_y h^3}{3EI} \tag{3}$$

$$H_y = \left(\sigma_y - \frac{P}{A}\right)\frac{S}{h} \tag{4}$$

where H_y is the lateral yield load and *A*, *I*, *S*, *h*, and σ_y, respectively, are the cross-sectional area, moment of inertia, and elastic section modulus, height of the column, and yield stress of the material [3].

2.2 Finite Element Model Validation

As illustrated in Fig. 2, the hysteretic behavior of the tested column, in both lateral *x* and *z* directions, obtained from the analysis is compared to the experimental results in the literature [12,15]. The FE analysis results in sloid line and the experimental results depicted with dashed line. H_y and δ_y, respectively, are the lateral yield load and the yield displacement. In both *x* and *z* directions, the FE analysis results have a reasonable agreement with the experimental results. The ultimate strength of the column is predicted with 1% error in *x* direction (FEM: H_{xmax}/H_y = 1.167, Experiment: H_{xmax}/H_y = 1.160, see Fig. 2a) and less than 5% in *z* direction (FEM: H_{zmax}/H_y = 1.123, Experiment: H_{zmax}/H_y = 1.174, see Fig. 2b).

In conclusion, the adopted finite element model, is able to capture the structural behavior of thin-walled steel square box columns with a reasonable accuracy considering the local buckling under constant axial force and circular bidirectional cyclic lateral loading. As shown in Fig. 3, buckling shape of the FE analysis at the end of analysis (see Fig. 3b) is captured relatively well compared to the experimental buckling deformation [12,15] (see Fig. 3a). In both the experiment and analysis, the column buckled inward and outward near the base of the column.

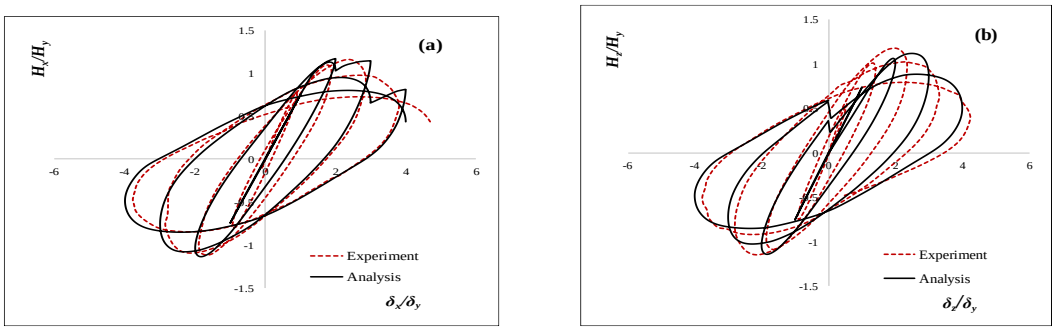

Fig. 2 - Hysteretic Behavior of the Tested Column.

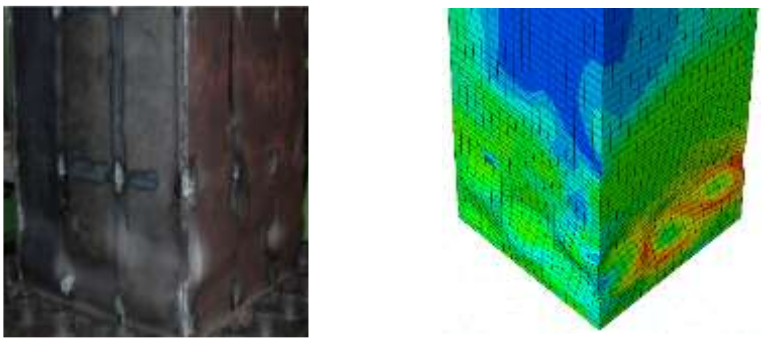

(a) Experiment [35] (b) FE Analysis

Fig. 3 - Buckling Deformation of the Tested Column.

3 Thin-Walled Steel Column with Graded Thickness

In a recent study [3], Al-Kaseasbeh and Mamghani (2019) have introduced and examined, under constant axial force and unidirectional cyclic lateral loading, the hysteretic behavior of a graded-thickness thin-walled steel square box column to inhibit the local buckling near the base of the column. The proposed BGB column has the same size and volume of material of the uniform BB column. As shown in Fig. 4c, the BGB column is divided into three segments of constant cross sections along its height. The first two segments from the base have the same height, which is equal to the size of cross- section (D) of the BB column. The upper segment has a height of h-2D, where h and D are same for both BB and BGB columns. In the proposed BGB column (see Fig. 4d), the first and second segments, respectively, have a thickness of 1.25t, and t, where t is the thickness of the BB column. The thickness of the upper segment, t_3, is calculated by equating the volume of material in both BB and BGB columns. The above configuration of the BGB column was chosen based on failure pattern of the tested columns in the literature [26]. As listed in Table 1, the same material and geometrical properties (except the plate thickness) are the same for both of the BB and BGB columns which are assumed to be made of the same carbon steel ASTM A242 [27]. For both BB and BGB columns, the same FEM details of the tested column, except the FE meshing, are used, as shown in Fig. 4b. For computational efficiency, the upper part of the column, height of h-2D, is divided into B31 elements with size of 90 mm. The height of the bottom half of the lower part of the column (equal to the width of cross-section, D) is divided into 30 S4R elements, while the remaining height (D) is only divided into 20 elements. Finally, each longitudinal stiffeners and subpanel between the stiffeners, respectively, have 3 and 6 columns of S4R elements.

4 Hysteretic Behavior of BB and Proposed BGB Columns

In order to investigate the hysteretic behavior of BB and BGB columns under constant axial force and bidirectional cyclic lateral loading, FE analyses were conducted using the substantiated FEM. Under the

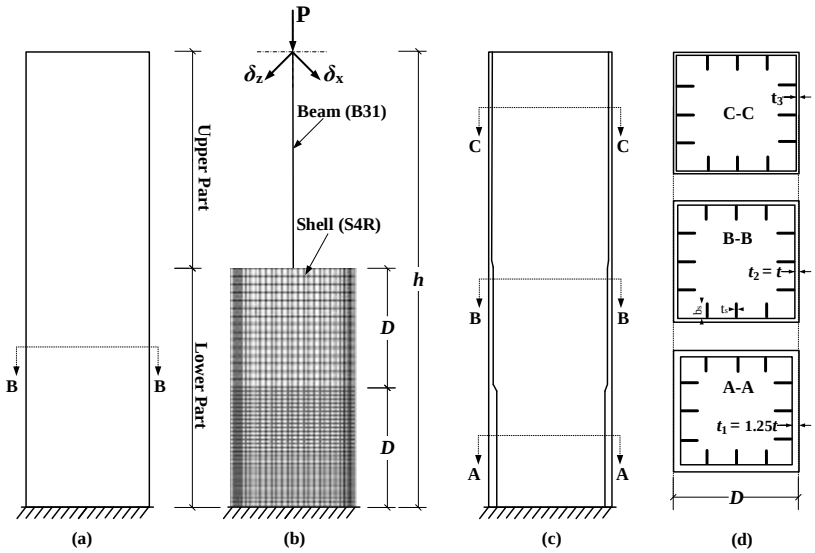

Fig. 4 - (a) BB Column, (b) FE Meshing, (c) BGB Column, and (d) Graded-thickness Sections.

bidirectional circular cyclic lateral loading, the applied displacement is equal in both lateral *x* and *z* directions. Consequently, the BB and BGB columns exhibit isotropic response in both *x* and *z* directions (e.g., see the results in Figs. 2a and 2b). In this paper, for brevity purpose, the results in the *z* direction are presented in the further analysis. As an example, for four pairs of BB and BGB columns, the normalized lateral load vs. lateral displacement hysteresis loops are shown in Fig. 5. The plotted hysteresis loops indicate a remarkable strength and ductility improvement in the proposed BGB columns. As compared to their BB column counterparts, the post-buckling behavior of the BGB columns is also improved. For instance, the normalized ultimate strength (i.e., H_{zmax}/H_y = 1.56) and the corresponding normalized maximum displacement (i.e. δ_{zm}/δ_y = 2.64) of BGB1 column, respectively, are 32% and 36% greater than those of the BB1 column as shown in Fig. 5a. In the BB1 column, the local buckling initiated earlier, where δ_{zm}/δ_y = 1.93, than the BGB1 column. A similar behavior exists in the all analyzed BB and BGB columns, as shown in Fig. 5. As shown in Fig. 6, the buckling shape of the proposed BGB1 column (see Fig. 6b) suffered less severe damage in its both flange and web compared to the conventional BB1 column (see Fig. 6a), and similar buckling behavior is observed in the all other BB and BGB columns. The previous comparison indicated the superior behavior in the proposed BGB columns over the uniform BB columns.

5 Loading Path Effect

A comparison between unidirectional, previous study by Al-Kaseasbeh and Mamaghani (2019) [3], and bidirectional loading conditions is conducted to highlight the effect of the cyclic loading pattern on the hysteretic behavior of thin-walled steel square box columns. Fig. 7 shows the hysteretic behavior of the uniform B and BB columns and graded-thickness GB and BGB columns under unidirectional and circular bidirectional cyclic lateral loading. The comparison indicates that the hysteresis loops under bidirectional circular cyclic lateral loading is totally different from those under unidirectional lateral cyclic loading. At the same amplitude of applied displacement, bidirectional loading pattern significantly causes more degradation in the strength and ductility of the column with the same material and structural parameters than unidirectional loading pattern. The significant deterioration is due to the accelerated local buckling under bidirectional circular cyclic lateral loading. To make a quantitative comparison between of the hysteretic behavior of the thin-walled steel square box columns under unidirectional and bidirectional circular loading conditions, the normalized loading path (i.e., H_x/H_y-H_z/H_y path for bidirectional loading) of BB and BGB columns are plotted as shown in Fig. 8. In addition, the ultimate strength of B column (H_{max}/H_y = 1.328) and GB column (H_{max}/H_y = 1.644) under one-cycle unidirectional cyclic lateral loading is also superimposed as a circular envelope on the Fig. 8 with a dashed and dash-dot lines, respectively. The ultimate strength

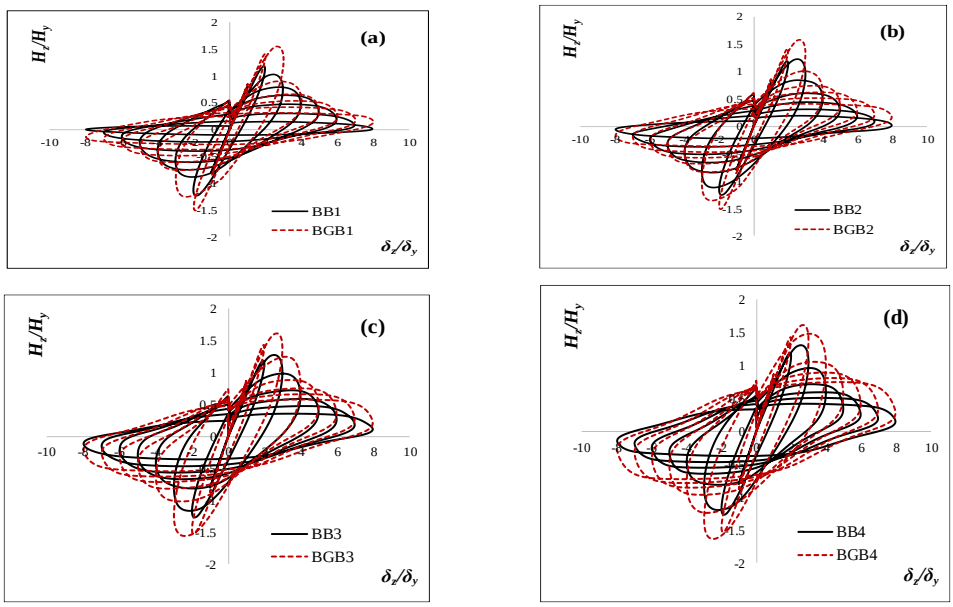

Fig. 5 - Comparison of Hysteretic Loops in *z* direction of: (a) BB1 vs. BGB1, (b) BB2 vs. BGB2, (c) BB3 vs. BGB3, (d) BB4 vs. BGB4.

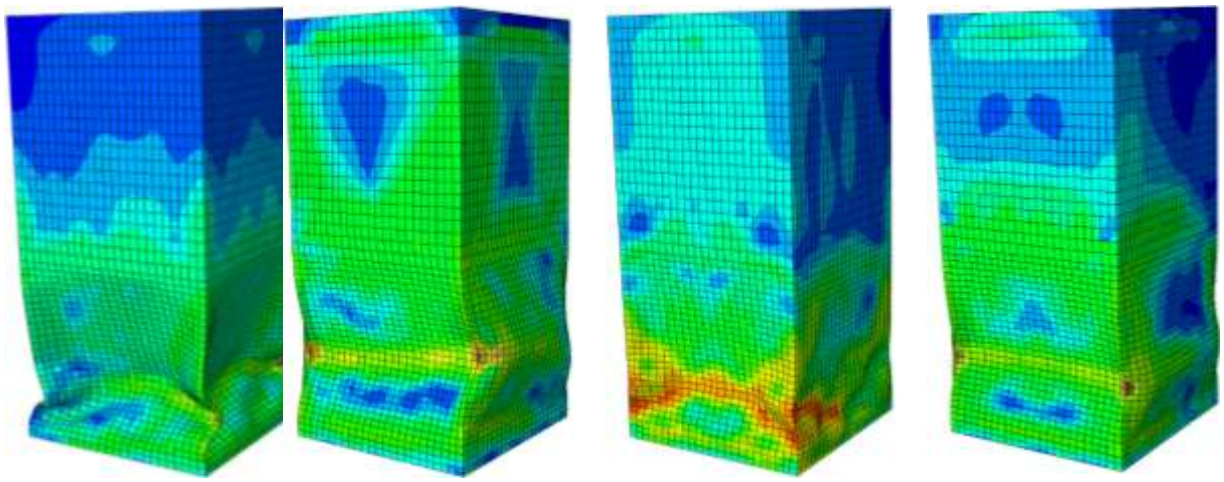

(a) Column BB1 (b) Column BGB1 (c) Column B1[3] (d) Column GB1[3]

Fig. 6 - Buckling shape of Columns.

difference is 13% (B vs. BB) and 6% (BG vs. BGB) between unidirectional and bidirectional circular cyclic lateral loading. Therefore, the hysteretic behavior of thin-walled steel square box columns under unidirectional loading is over-simplified and leads to over-estimated strength and ductility capacity.

5.1 Buckling Deformations

Fig. 6 compares the buckling deformations of the columns at the end of the analysis. The comparison visually indicates that the BB column (δ_m/δ_y = 1.93) (see Fig. 6a) and BGB column (δ_m/δ_y = 2.64) (see Fig. 6b), under bidirectional loading, buckled earlier than the B column (δ_m/δ_y = 2.28) (see Fig. 6c) and GB column (δ_m/δ_y = 3) (see Fig. 6d) under unidirectional loading. Furthermore, the magnitude of the local buckling seems more critical under bidirectional circular loading. As opposed to the unidirectional cyclic

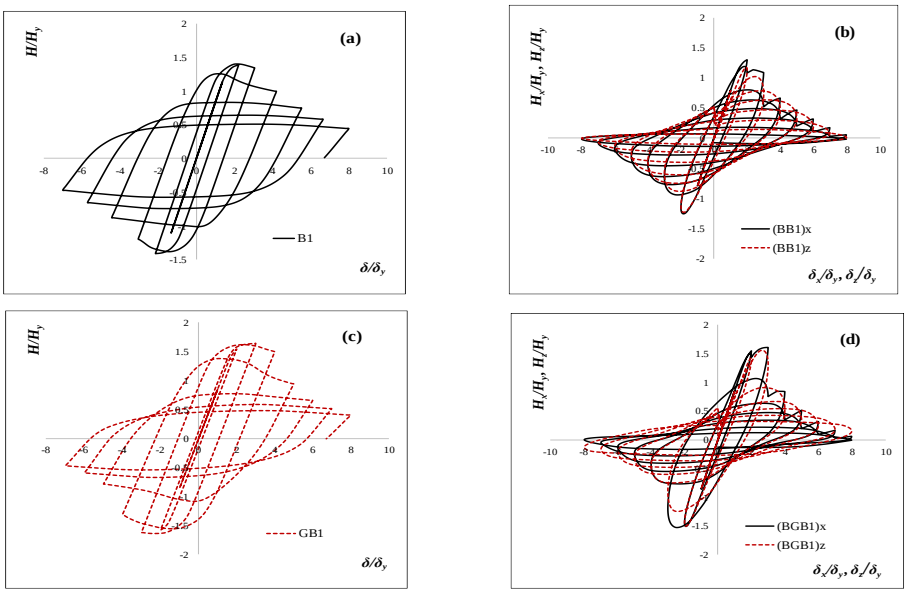

Fig. 7 - Hysteretic Loops; (a) uniform-thickness column under uniaxial lateral loading (B1), (b) uniform-thickness column under biaxial lateral loading (BB1), (c) graded-thickness column under uniaxial lateral loading (GB1), (d) graded-thickness column under biaxial lateral loading (BGB1).

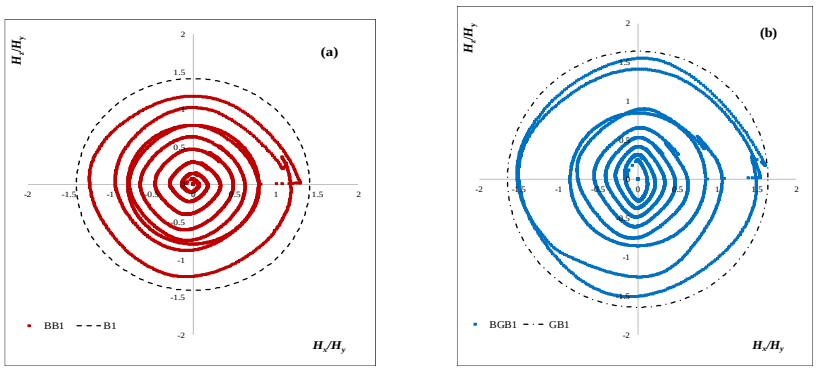

Fig. 8 - Loading Paths of Columns: (a) BB1 vs. B1 Columns, and (b) BGB1 vs. BG1 Columns.

lateral loading, it is believed that because all the plates of the column are subjected to compression loading all the time of the analysis under bidirectional circular cyclic lateral loading.

5.2 Energy Absorption Capacity

In order to predict the strength degradation, the dissipated energy of the column is investigated and presented in Fig. 9. The cumulative dissipated energy is calculated as the sum of the enclosed area under the normalized hysteretic loops in x and z direction for bidirectional circular loading and in x direction for unidirectional loading. As observed in Fig. 9, the columns with same material and geometrical properties, dissipate more energy under the bidirectional circular cyclic lateral loading than those under unidirectional cyclic lateral loading which, in turns, results in a degradation in the strength and ductility of the column.

6 Parametric Study

A parametric study was carried out to provide insight into the effect of key design parameters including: flange width-to-thickness ratio parameter (R_f), column slenderness ratio parameter (λ), magnitude of axial

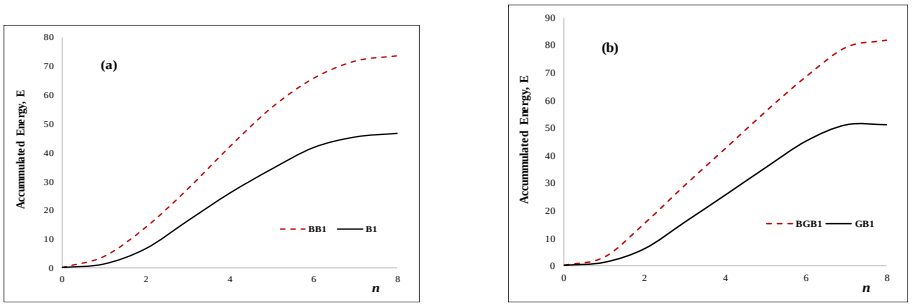

Fig. 9 - Energy Absorption Capacity of Columns.

load (P/P_y), and number of loading cycles (N), on the overall inelastic structural behavior of the BB and BGB columns. The practical range of these design parameters of thin-walled steel square box bridge piers are: $0.3 \leq R_f \leq 0.5$, $0.2 \leq \lambda \leq 0.5$ [28]. For thin-walled steel stiffened square box columns, diaphragms are usually installed at an interval smaller than the pier width (D), $\alpha = a/D \leq 1.0$, where a is the distance between diaphragms [28]. As listed in Table 1, a total of 38 columns is analyzed using the adopted FEM in ABAQUS/Standard [21]. The studied range of these parameters are: R_f varying from 0.26 to 0.56, λ with a range of 0.26 - 0.5, the axial load ratio, P/P_y, where five different ratios (i.e., P/P_y = 0.1, 0.122, 0.15, 0.20, and 0.3) are applied on BB5 and BGB5 columns. To investigate the effect of the number of loading cycles at each displacement amplitude (N), the BB1 and BGB1 columns were analyzed under both one ($N= 1$), and three ($N= 3$) cycles at each displacement level.

6.1 Effect of Width-to-Thickness Ratio Parameter (R_f)

The effect of the R_f on the hysteretic behvior of the column was investigated. The increase in R_f is either due to an increase in the width of the column or a decrease in its flange plate thickness. In this study, the side width of the BB and BGB columns kept constant and the thickness is changed. As shown in Fig. 10, the envelope curves of the normalized lateral load vs. lateral displacement relation for both BB and BGB columns with different R_f values are plotted. The H_{zmax}/H_y and δ_{zm}/δ_y of both BB and BGB columns are improved by decreasing R_f and keeping the other column's parameter unchanged. For instance, the H_{zmax}/H_y and δ_{zm}/δ_y , respectively, are increased by 11% and 33% as R_f is decreased from 0.56 (column BB1) to 0.26 (column BB5) with λ = 0.26 (see Fig. 10a). In a similar way, as shown in Fig. 10c, H_{zmax}/H_y and δ_{zm}/δ_y are increased by 4% and 2%, respectively, as the R_f decreases from 0.56 (column BGB1) to 0.26 (column BGB5). After the peak point, the post-buckling curve is less steep as R_f gets smaller and the column experiences higher ductile behavior.

6.2 Effect of Slenderness Ratio Parameter (λ)

The λ effect on the hysteretic behavior of both BB and BGB columns was studied. The H_{zmax}/H_y and δ_{zm}/δ_y of both BB and BGB columns improve as λ gets smaller as shown in Fig. 11. For example, the H_{zmax}/H_y and δ_{zm}/δ_y, with R_f = 0.26, are increased by 10% and 36%, respectively, as λ decreases from 0.5 (column BB15) to 0.26 (column BB5) as shown in Fig. 11b. In the BGB columns, the H_{zmax}/H_y and δ_{zm}/δ_y are improved by 21% and 40%, respectively, as λ decreases from 0.5 (column BGB15) to 0.26 (column BGB5) as shown in Fig. 11d. After the peak point, the post-buckling curve slope gets steeper, and the area enclosed by the envelope curve decreases when λ is higher. The same behavior exists in all other analyzed columns with different R_f values.

6.3 Strength and Ductility Evaluation of BB and BGB Columns

Using the computed ultimate strength and ductility of both BB and BGB columns the design equation are derived based on the normalized strength H_{zmax}/H_y and integrated parameters $(1+P/P_y)\ R_f\ \lambda$, considering the interaction of R_f, λ, and P/P_y on the strength of the column. The Equations 5 and 6, respectively, are the best fitting equations to the computed ultimate strength of BB and BGB columns.

Table 1 - Material and Geometrical Properties of BB and BGB Columns.

BB Columns						BGB Columns							
Column	*h(mm)*	*t(mm)*	R_f	λ	P/P_y	Column	*h(mm)*	*t (mm)*			R_f	λ	P/P_y
								t_1	t_2	t_3			
BB1	3403	9.00	0.56	0.26	0.122	**BGB1**	3403	11.25	9.00	7.75	0.56	0.26	0.122
BB2	3403	11.00	0.46	0.26	0.122	**BGB2**	3403	13.75	11.00	9.46	0.46	0.26	0.122
BB3	3403	14.00	0.36	0.26	0.122	**BGB3**	3403	17.50	14.00	12.00	0.36	0.26	0.122
BB4	3403	16.90	0.30	0.26	0.122	**BGB4**	3403	21.14	16.90	14.55	0.30	0.26	0.122
BB5	3403	19.50	0.26	0.26	0.122	**BGB5**	3403	24.40	19.50	16.80	0.26	0.26	0.122
BB5-10	3403	19.50	0.26	0.26	0.100	**BGB5-10**	3403	24.40	19.50	16.80	0.26	0.26	0.100
BB5-15	3403	19.50	0.26	0.26	0.150	**BGB5-15**	3403	24.40	19.50	16.80	0.26	0.26	0.150
BB5-20	3403	19.50	0.26	0.26	0.200	**BGB5-20**	3403	24.40	19.50	16.80	0.26	0.26	0.200
BB5-30	3403	19.50	0.26	0.26	0.300	**BGB5-30**	3403	24.40	19.50	16.80	0.26	0.26	0.300
BB6	3920	9.00	0.56	0.30	0.122	**BGB6**	3920	11.25	9.00	8.00	0.56	0.30	0.122
BB7	3920	11.00	0.46	0.30	0.122	**BGB7**	3920	13.00	11.00	9.36	0.46	0.30	0.122
BB8	3920	14.00	0.36	0.30	0.122	**BGB8**	3920	16.25	14.00	11.65	0.36	0.30	0.122
BB9	3920	16.90	0.30	0.30	0.122	**BGB9**	3920	21.14	16.90	15.13	0.30	0.30	0.122
BB10	3920	19.50	0.26	0.30	0.122	**BGB10**	3920	16.25	19.50	11.65	0.26	0.30	0.122
BB11	6530	9.00	0.56	0.50	0.122	**BGB11**	6530	11.25	9.00	8.60	0.56	0.50	0.122
BB12	6530	11.00	0.46	0.50	0.122	**BGB12**	6530	13.00	11.00	9.96	0.46	0.50	0.122
BB13	6530	14.00	0.36	0.50	0.122	**BGB13**	6530	16.25	14.00	12.40	0.36	0.50	0.122
BB14	6530	16.90	0.30	0.50	0.122	**BGB14**	6530	21.14	16.90	16.11	0.30	0.50	0.122
BB15	6530	19.50	0.26	0.50	0.122	**BGB15**	6530	21.75	19.50	16.60	0.26	0.50	0.122

For all columns: Width of cross-section *(D)* = 900 mm, $t_s / b_s / l$ = *6/ 80/ 225 mm*. σ_y = 378.6 MPa, *E* = 206 GPa, and, ν = 0.3.
Columns BB3 and BGB3 are loaded with one-cycle (*N* = 1) and three-cycle (*N* = 3).
$P_y = \sigma_y * A$, $A = (D^2 - D_i^2)$, $D_i = D - 2t$, *t* = Plate thickness for the B column.
I = moment of inertia = $(D^4 - D_i^4)/12$, *S* = elastic section modulus = $(D^4 - D_i^4)/6D$.

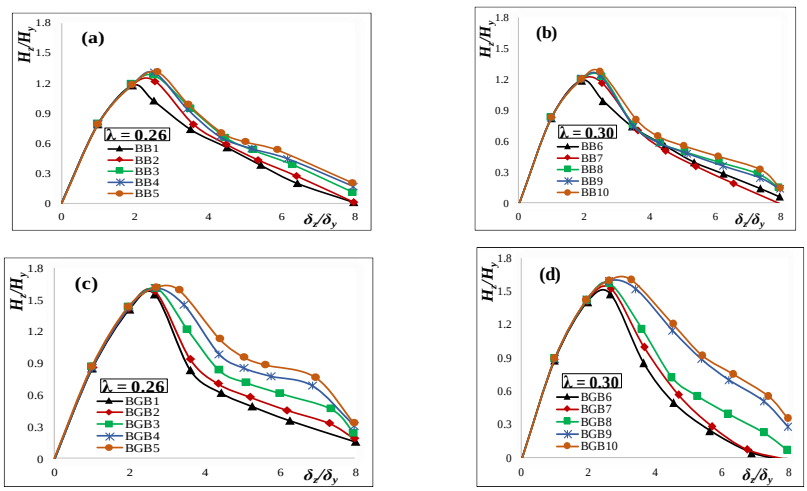

Fig. 10 - Effect of R_f on Hysteretic Behavior of: (a) BB columns with λ = 0.26, (b) BB columns with λ = 0.3, (c) BGB columns with λ = 0.26, and (d) BGB columns with λ = 0.3.

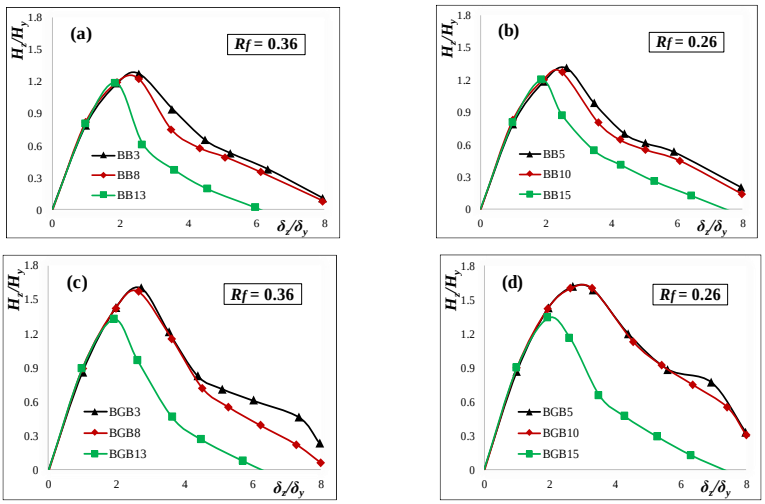

Fig. 11 - Effect of λ on Hysteretic Behavior of: (a) BB columns with R_f = 0.36, (b) BB columns with R_f = 0.26 (c) BGB columns with R_f = 0.36, and (d) BGB columns with R_f = 0.26.

$$\frac{H_{z\max}}{H_y} = \frac{1.017}{\left[\left(1+\frac{P}{P_y}\right)R_f\lambda\right]^{0.092}} \qquad \text{BB Columns} \qquad (5)$$

$$\frac{H_{z\max}}{H_y} = \frac{1.002}{\left[\left(1+\frac{P}{P_y}\right)R_f\lambda\right]^{0.201}} \qquad \text{BGB Columns} \qquad (6)$$

For both BB and BGB columns, an improvement in the ultimate strength is observed when integrated parameters $(1+P/P_y)\ R_f\ \lambda$ decrease. In this study, the failure of thin-walled steel columns is set to occur when the displacement equals either δ_{zm} or $\delta_{z0.9}$. The δ_{zm} is the displacement corresponding to H_{zmax}/H_y while the $\delta_{z0.9}$ is defined as the displacement where the post-peak strength drops to 90% of H_{zmax}/H_y [2,3,26]. The ductility factors (i.e., δ_{zm}/δ_y and $\delta_{z0.9}/\delta_y$) are key parameters in the evaluation of the ductile behavior of both BB and BGB columns. As the strength significantly deteriorates after the peak point due to the local buckling, it is reasonable to use the $\delta_{z0.9}/\delta_y$ parameter to evaluate ductility of the columns [2,3,10,26]. For both BB and BGB columns, the axial load effect was not considered for the fitting equations of δ_{zm}/δ_y parameter, while it is included in the equations of $\delta_{z0.9}/\delta_y$ parameter. The applicable restrictions of these formulae are $0.26 \le R_f \le 0.56$, $0.26 \le \lambda \le 0.5$, and $P/P_y \le 0.3$. It is worth mentioning that nonlinear least-squares regression was used for the curve fitting. The proposed formulae that fit the computed δ_{zm}/δ_y and $\delta_{z0.9}/\delta_y$ values of the analyzed columns are as follows:

$$\frac{\delta_{z\mathrm{m}}}{\delta_y} = \frac{1.183}{\left[R_f\lambda\right]^{0.306}} \qquad \text{BB Columns} \qquad (7)$$

$$\frac{\delta_{z0.9}}{\delta_y} = \frac{1.332}{\left[\left(1+\frac{P}{P_y}\right)R_f\lambda\right]^{0.315}} \qquad \text{BGB Columns} \qquad (8)$$

$$\frac{\delta_{zm}}{\delta_y} = \frac{1.257}{\left[R_f \lambda\right]^{0.325}} \tag{9}$$

$$\frac{\delta_{z0.9}}{\delta_y} = \frac{1.185}{\left[\left(1+\frac{P}{P_y}\right) R_f \lambda\right]^{0.447}} \quad \text{BGB Columns} \tag{10}$$

7 Conclusions

This paper dealt with evaluating the hysteretic behavior of the uniform (BB) and proposed graded-thickness (BGB) thin-walled steel square box columns under constant axial force and circular bidirectional cyclic lateral loading. The following conclusions are summarized:

- The validity of adopted FEM in capturing the cyclic elastoplastic behavior of the column, under constant axial force and circular bidirectional cyclic lateral loading, is verified with experimental results reported in the literature.
- The proposed BGB column with size and volume of material equivalent to the uniform BB column, under constant axial force and circular bidirectional cyclic lateral loading, is proved to have a superiority and significant improvement in the overall hysteretic behavior compared to counterpart of the BB column. In overall, the ultimate strength of BGB column was increased at an average of 28% when λ, respectively, equals 0.26 and 0.3. In the case of λ = 0.5, the ultimate strength was improved by only 11% in comparison with BB columns.
- For BB and BGB columns with the same material and geometrical properties, bidirectional cyclic lateral loading significantly leads to degradation in strength and ductility at the same amplitude of displacement. In addition, more damage and dissipated energy were reported under bidirectional loading. Therefore, the hysteretic behavior of thin-walled steel square box columns under unidirectional loading is over-simplified and leads to over-estimated strength and ductility capacity.
- The strength and ductility of BB and BGB column were improved by decreasing R_f and λ parameters. Furthermore, the increasing P/P_y and N at each displacement level causes more deterioration in the overall hysteretic behavior of the column after the peak point.
- In order to predict the ultimate strength and ductility of BB and BGB columns, design formulae have been derived based on a conducted parametric study.

7. References

[1] Bedair O (2015): Novel Design Procedures for Rectangular Hollow Steel Sections Subject to Compression and Major and Minor Axis Bending. *Pract Period Struct Des Constr*; ASCE, SC.1943-5576.0000248.

[2] Al-Kaseasbeh Q, Mamaghani IHP (2018): Buckling Strength and Ductility Evaluation of Thin-Walled Steel Tubular Columns with Uniform and Graded Thickness under Cyclic Loading. *ASCE, Journal of Bridge Engineering*, ASCE, BE.1943-5592.0001324.

[3] Al-Kaseasbeh Q, Mamaghani IHP (2019): Buckling strength and ductility evaluation of thin-walled steel stiffened square box columns with uniform and graded thickness under cyclic loading. *Engineering Structures*; j.engstruct.2019.02.026.

[4] Goto Y, Mizuno K, Prosenjit Kumar G (2012): Nonlinear Finite Element Analysis for Cyclic Behavior of Thin-Walled Stiffened Rectangular Steel Columns with In-Filled Concrete. *J Struct Eng*, ASCE:ST.1943-541X.0000504.

[5] McCormick J (2018): Considerations for Use of HSS in Seismic Frame Systems - Hollow Structural Sections https://steeltubeinstitute.org/hss/2018/09/04/considerations-for-use-of-hss-in-seismic-frame-systems/.

[6] Aoki T, Susantha KAS (2005): Seismic Performance of Rectangular-Shaped Steel Piers under Cyclic Loading.

J Struct Eng 2005;131:240–9. doi:10.1061/(ASCE)0733-9445(2005)131:2(240).

[7] Ge H, Gao S, Usami T (2000): Stiffened steel box columns. Part 1: Cyclic behaviour. *Earthq Eng Struct Dyn* doi:10.1002/1096-9845(200011)29:11<1691::AID-EQE989>3.0.CO;2-U.

[8] Mamaghani IHP, Usami T, Mizuno E (1996): Cyclic elastoplastic large displacement behaviour of steel compression members. *J Struct Eng, JSCE* ;42:135–45.

[9] Mamaghani IHP, Usami T, Mizuno E (1997): Hysteretic behavior of compact steel box beam-columns. *J Struct Eng JSCE*, Japan 1997;43A:187–94.

[10] Gao S, Usami T, Ge H (1998): Ductility Evaluation of Steel Bridge Piers with Pipe Sections. *J Eng Mech*, doi:10.1061/(ASCE)0733-9399(1998)124:3(260).

[11] Mamaghani IHP, Packer JA (2002): Inelastic behaviour of partially concrete-filled steel hollow sections. *4th Struct. Spec. Conf.*, 2002, p. 1–10.

[12] Dang J, Yuan H, Igarashi A, Aoki T (2017): Multiple-Spring Model for Square-Section Steel Bridge Columns under Bidirectional Seismic Load. *J Struct Eng*, doi:10.1061/(ASCE)ST.1943-541X.0001735.

[13] Watanabe E, Sugiura K, Oyawa W (2000): Effects of multi-directional displacement paths on the cyclic behaviour of rectangular hollow steel columns. *Doboku Gakkai Ronbunshu*, pp. 79–95.

[14] Anderson EL, Mahin S.A (2004): An Evaluation of Bi-Directional Earthquake Shaking on the Provisions of the AASHTO Guide Specifications for Seismic Isolation Design. *Proc. 13th World Conf. Eq.* Eng, 2004.

[15] Aoki T, Ohnishi A, Suzuki M (2007): Experimental Study on the Seismic Resistance Performance of Rectangular Cross Section Steel Bridge Piers Subjected to Bi-Directional Horizontal Loads. *Doboku Gakkai Ronbunshuu*, doi:10.2208/jsceja.63.716.

[16] Dang J, Aoki T (2013): Bidirectional loading hybrid tests of square cross-sections of steel bridge piers. *Earthq Eng Struct Dyn*, doi:10.1002/eqe.2262.

[17] Goto Y, Koyama R, Fujll Y, Obata M (2009): Ultimate State of Thin-Walled Stiffened Rectangular Steel Columns under Bi-Directional Seismic Excitations. *Doboku Gakkai Ronbunshuu*, doi:10.2208/jsceja.65.61.

[18] Goto Y, Jiang K, Obata M (2006): Stability and Ductility of Thin-Walled Circular Steel Columns under Cyclic Bidirectional Loading. *J Struct Eng*, doi:10.1061/(ASCE)0733-9445(2006)132:10(1621).

[19] Onishi A, Aoki T, Suzuki M (2005): Experimental study on the seismic resistance performance of steel bridge subjected to bi-directional horizontal loads. *Bull Aichi Inst Tech*; 40:121–9.

[20] Nishikawa K, Yamamoto S, Natori T, Terao K, Yasunami H, Terada M (1998): Retrofitting for seismic upgrading of steel bridge columns. *Eng Struct*, doi:10.1016/S0141-0296(97)00025-4.

[21] Hibbit, Karlsson, Sorensen. ABAQUS 2014 Documentation 2014.

[22] Chen S, Xie X, Zhuge H (2019): Hysteretic model for steel piers considering the local buckling of steel plates. *Eng Struct*, doi:10.1016/j.engstruct.2018.12.101.

[23] Banno S, Mamaghani IHP, Usami T, Mizuno E (1998): Cyclic Elastoplastic Large Deflection Analysis of Thin Steel Plates. *J Eng Mech, ASCE*; doi:10.1061/(ASCE)0733-9399(1998)124:4(363).

[24] Ucak A, Tsopelas P (2012): Accurate modeling of the cyclic response of structural components constructed of steel with yield plateau. *Eng Struct*, doi:10.1016/j.engstruct.2011.10.015.

[25] Hassan MS, Salawdeh S, Goggins J (2018): Determination of geometrical imperfection models in finite element analysis of structural steel hollow sections under cyclic axial loading. *J Constr Steel Res* doi:10.1016.

[26] Usami T. (1996): Interim guidelines and new technologies for seismic design of steel structures. *Comm. New Technol. Steel Struct. JSCE*, Tokyo (in Japanes).

[27] ASTM. ASTM A242 / A242M-13(2018): Standard Specification for High-Strength Low-Alloy Structural Steel. *ASTM Int West Conshohocken*, PA, doi:10.1520/A0242_A0242M-13R18.

[28] Chen WF, Duan L (2014) : Bridge Engineering Handbook, 2nd Edition, Seismic Design. CRC Press; 2014. doi:10.1201/b15616.

